

Pressure-induced changes in the electron density distribution in α -Ge near the α - β transition

Rui Li, Jing Liu, Ligang Bai, John S. Tse, and Guoyin Shen

Citation: [Applied Physics Letters](#) **107**, 072109 (2015); doi: 10.1063/1.4929368

View online: <http://dx.doi.org/10.1063/1.4929368>

View Table of Contents: <http://scitation.aip.org/content/aip/journal/apl/107/7?ver=pdfcov>

Published by the [AIP Publishing](#)

Articles you may be interested in

[Pressure-induced structural changes in NH₄Br](#)

J. Chem. Phys. **143**, 064505 (2015); 10.1063/1.4927782

[Pressure-induced kinetics of the \$\alpha\$ to \$\omega\$ transition in zirconium](#)

J. Appl. Phys. **118**, 025902 (2015); 10.1063/1.4926724

[High pressure Laue diffraction and its application to study microstructural changes during the \$\alpha \rightarrow \beta\$ phase transition in Si](#)

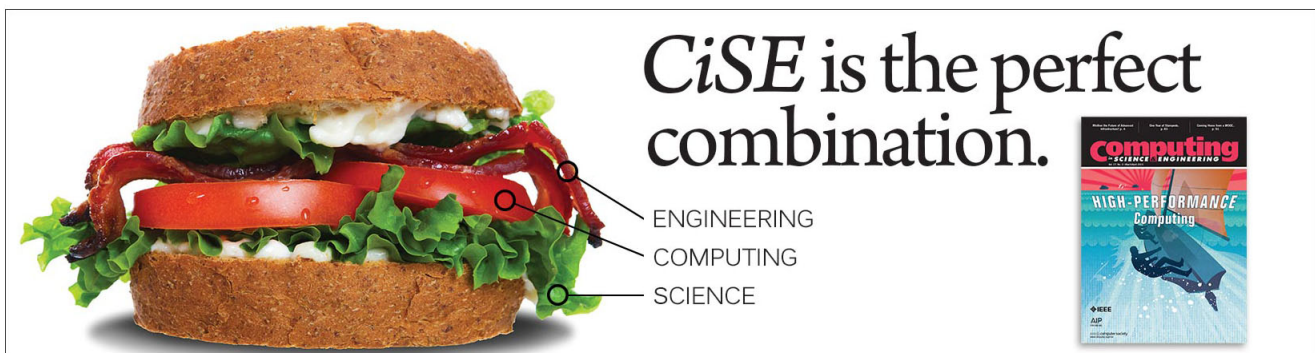
Rev. Sci. Instrum. **86**, 072204 (2015); 10.1063/1.4926894

[Pressure-induced structures of Si-doped HfO₂](#)

J. Appl. Phys. **117**, 234102 (2015); 10.1063/1.4922717

[Pressure-induced pseudoatom bonding collapse and isosymmetric phase transition in Zr₂Cu: First-principles predictions](#)

J. Chem. Phys. **139**, 234504 (2013); 10.1063/1.4846995

The advertisement for CiSE (Computing in Science and Engineering) features a large image of a sandwich on the left. The sandwich is filled with lettuce, tomato, and meat. Three lines with circular endpoints point from the sandwich to the text 'ENGINEERING', 'COMPUTING', and 'SCIENCE' on the right. To the right of the sandwich is the text 'CiSE is the perfect combination.' in a large, serif font. Further to the right is a small image of a journal cover titled 'Computing in Science and Engineering' with the subtitle 'HIGH-PERFORMANCE Computing' and an image of a blue submarine.

Pressure-induced changes in the electron density distribution in α -Ge near the α - β transition

Rui Li,^{1,2,3} Jing Liu,¹ Ligang Bai,² John S. Tse,⁴ and Guoyin Shen^{2,a)}

¹Institute of High Energy Physics, Chinese Academy of Sciences, Beijing 100049, China

²HPCAT Geophysical Laboratory, Carnegie Institution of Washington, Argonne, Illinois 60439, USA

³University of Chinese Academy of Sciences, Chinese Academy of Sciences, Beijing 100049, China

⁴Department of Physics and Engineering Physics, University of Saskatchewan, Saskatoon, Saskatchewan S7N 5E2, Canada

(Received 18 June 2015; accepted 11 August 2015; published online 19 August 2015)

Electron density distributions in α -Ge have been determined under high pressure using maximum entropy method with structure factors obtained from single crystal synchrotron x-ray diffraction in a diamond anvil cell. The results show that the sp^3 bonding is enhanced with increasing pressure up to 7.7(1) GPa. At higher pressures but below the α - β transition pressure of 11.0(1) GPa, the sp^3 -like electron distribution progressively weakens with a concomitant increase of d -orbitals hybridization. The participation of d -orbitals in the electronic structure is supported by Ge $K\beta_2$ ($4p$ - $1s$) x-ray emission spectroscopy measurements showing the reduction of $4s$ character in the valence band at pressures far below the α - β transition. The gradual increase of d -orbitals in the valence level in the stability field of α -Ge is directly related to the eventual structural transition.

© 2015 AIP Publishing LLC. [<http://dx.doi.org/10.1063/1.4929368>]

Pressure-induced phase transition in Ge from diamond structure to β -tin structure is representative as a type of covalent-metallic transitions often found in group IV elements (Si, Ge, α -Sn), III-V compounds (AlSb, GaP, GaAs, GaSb, InP, InAs, InSb), and II-VI compounds (ZnS, ZnSe, ZnTe, CdTe).¹⁻⁶ These transformations are accompanied by large volume collapses and changes in the bonding with increased metallic character.^{6,7} In the metallic high-pressure phases, an important feature is the participation of d electrons in bonding^{7,8} at the expense of diminishing sp^3 directional bonds.⁹ Despite decades of effort, the question whether the hybridization of d -orbitals happens abruptly at the transition or appears progressively with the gradual decrease of covalent bonding with pressure before the transition still remains.

Low pressure Ge phase, often referred as α -Ge with space group $Fd\bar{3}m$, transforms to a tetragonal β -Ge with space group $I4_1/amd$ at a pressure around 11 GPa.¹⁰⁻¹² The Ge atoms in diamond structure are generally considered to be sp^3 -hybridized. There are several direct and indirect theoretical studies on the variation of the sp^3 bonding under pressure. However, the changes in the degree of sp^3 hybridization with pressure remain controversial. Bouarissa *et al.*¹³ calculated the pressure dependence of the energy gaps and electron density with the pseudopotential method and showed that the electron density along the bond direction decreases with increasing pressure. In comparison, an all-electron full potential linearized augmented plane-wave (LAPW) calculation showed that the sp^3 hybridization increases first with increasing pressure and then decreases under further compression.¹⁴ In experiments, the forbidden (222) reflection has been used for studying the valence bonding charge.^{15,16} For example, the intensity of the Si (222) reflection at high pressures displayed a sudden increase at

around 11 GPa,¹⁷ which is related to a precursor lattice of the β -tin phase.¹⁸ Therefore, the information on electron density distribution (EDD) is very useful in the characterization of the chemical bonds. However, the EDD data for Ge are currently limited to ambient pressure only¹⁹⁻²² and no pressure dependence of EDD is available.

In this letter, we report the EDD of α -Ge from synchrotron single-crystal x-ray diffraction (XRD) studies under high pressure using a diamond anvil cell (DAC). In combination with x-ray emission spectroscopy (XES) measurements, we show that the appearance of d -orbitals in α -Ge occurs at a pressure much lower than the structural α - β transition. It is found that the sp^3 covalent bonding increases initially with increasing pressure up to 7.7(1) GPa, above which the electron topology changes with progressively diminished sp^3 character and a gradual increase of d -hybridization in the valence orbitals.

Single-crystal XRD measurements were performed at the 16-BM-D beamline at the Advanced Photon Source (APS). A monochromatic beam of wavelength 0.35424(3) Å was focused to a beam size of about $5 \times 10 \mu\text{m}^2$ full-width-half-maximum (FWHM) in both horizontal and vertical directions, respectively. A high quality single crystal of Ge (Hefei Kejing Material Technology Co., Ltd., China) was cut into a rectangular piece of approximately $20 \times 30 \mu\text{m}^2$ and 7 μm in thickness, and subsequently loaded into a DAC with a large opening angle of $4\theta = 60^\circ$. The culet size of the anvils was 250 μm (Fig. 1(a)). A 250 μm Re gasket was pre-indented to 35 μm thick and a hole of 120 μm in diameter was drilled as the sample chamber. Neon was used as the pressure-transmitting medium. The DAC was loaded together with several small ruby balls for pressure determination using the ruby fluorescence method.²³ XRD images were collected by a MAR345 detector as the sample was rotated along a vertical axis perpendicular to the x-ray beam. A procedure using the ω -scan covering a range of 50° with a step of 2° was performed. Two independent runs

^{a)}Author to whom correspondence should be addressed. Electronic mail: gshen@ciw.edu

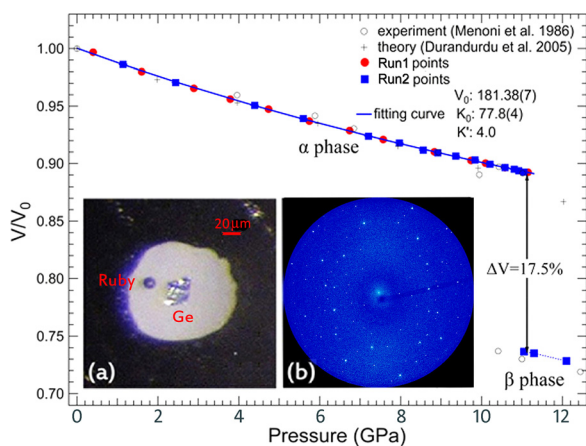


FIG. 1. The pressure-volume relation of Ge. The fit to the Birch-Murnaghan equation of state gives a bulk modulus $K_0 = 77.8(4)$ GPa with the pressure derivative K' fixed at 4.0. The single-crystal diffraction measurements provide high precision pressure-volume data, with error bars far less than the symbol sizes. The data are compared to theoretical calculations⁴⁰ and previous experimental results.¹² (a) A photograph of the sample configuration under microscope at 2.9 GPa. (b) A typical diffraction image at 2.9 GPa of single crystal data from the α -Ge sample in a diamond anvil cell.

were conducted in the pressure range from 0.6 to 12.0 GPa (Fig. 1). The α - β transition (Fig. 1, see also Fig. S1 in the supplementary material²⁴) was found to be sharp and accompanied by a large volume collapse of 17.5%.

Data integration and pixel by pixel reciprocal plane reconstructions were performed using the GSE_ADA software.²⁵ In the range of $\sin \theta/\lambda < 1.3 \text{ \AA}^{-1}$, 19 usable independent reflections were found using the searching procedure. Structural refinements were carried out using the SHELX²⁶ program with the R factor less than 2.3% (see Tables S1 and S2 in the supplementary material²⁴ for details). The analysis of the α -Ge was performed by the maximum entropy method (MEM)²⁷ using the software PRIMA²⁸ with the unit cell divided into $60 \times 60 \times 60$ pixels. To avoid bias, priors from

uniform density, superposition of atom densities (pro-crystal), and electron densities computed from theoretical LAPW calculations with the Wu-Cohen functional were used separately in the MEM calculations. No noticeable differences in the EDD derived from different priors were found. The resulting reliability factor on the structure factors R_{MEM} was set to be 1%. The derived three-dimensional (3D) and two-dimensional (2D) EDDs were visualized with the program VESTA.²⁹

To examine the effect of pressure on the electron topology, we have computed the difference of the EDD between two pressure points (Δ EDD). The 3D isosurfaces are shown in Fig. 2(a), and the integrated Δ EDDs between two successive pressure points along the [100] from the nuclei to the center of two atoms and [111] direction from the nuclei to the bonding center are shown in Figs. 2(b) and 2(c), respectively, for the two separate runs. The 3D isosurface shown on the far left corner of Fig. 2(a) is the difference of the EDD at 1.4 GPa from 4.6 GPa. It can be seen that electron densities are increased around Ge nuclei along the [111] direction by about 1.5 e/\AA^3 (Fig. 2(b)). From the Δ EDD of 7.7 GPa from 4.6 GPa, a similar increase in the electron density along [111] is observed. The trend indicates that sp^3 bonding increases with pressure up to 7.7 GPa (Fig. 2(a)). A comparison between Figs. 2(b) and 2(c) affirms this conclusion and demonstrates consistency between the two sets of experiments: the electron densities gain from initial pressure to 7.7 GPa along the [111] direction were 2.3 and 1.5 e/\AA^3 in the two runs, respectively (Figs. 2(b) and 2(c)). Above 7.7 GPa, the EDDs along [111] direction display gradual weakening. On the other hand, the EDDs along [100] direction increase gradually above 7.7 GPa. The Δ EDD of 9.0 GPa from 7.7 GPa (Fig. 2(a)) shows negative differences along [111] and the positive differences expanding to the [100] direction. These variations are even clearer from the Δ EDD of 10.6 GPa from 7.7 GPa (Fig. 2(a)). The suppression along [111] and the increase along [100] may be interpreted as the depopulation of sp^3 electrons and the hybridization with

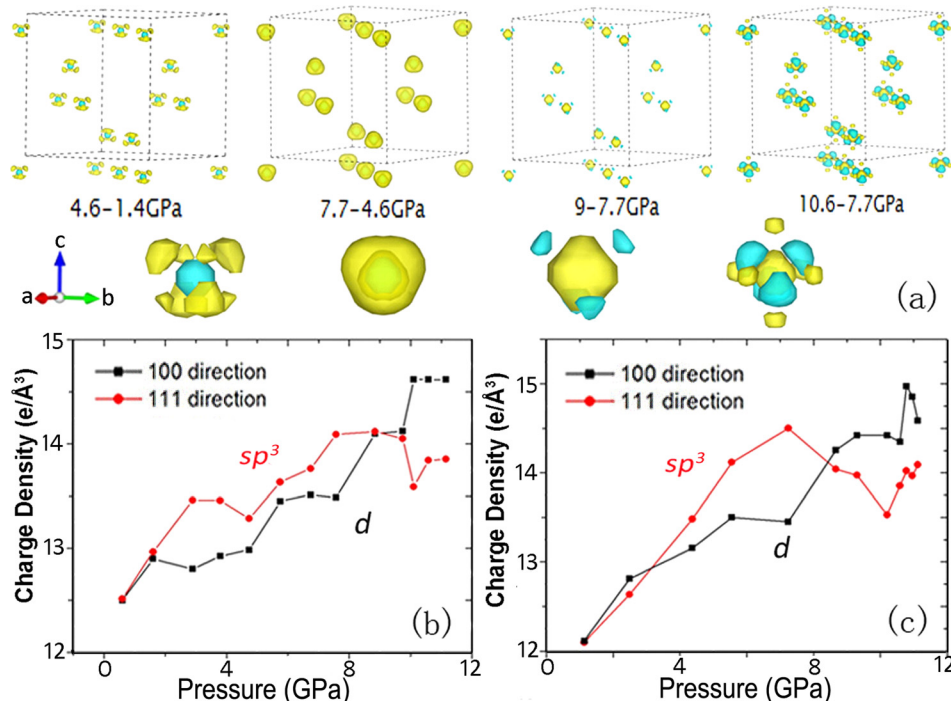


FIG. 2. Deformation EDDs between two pressure points. (a) The 3D isosurface maps of subtracted distributions. Also shown in (a) is the enlarged single atom isosurface maps, with the positive and negative differences displayed as yellow and blue. (b) and (c) Pressure dependences of the valence electron densities along [111] and [100] directions in two separate experimental runs, respectively. It can be seen that the electron density increases continuously with increasing pressure along [100] direction, while along [111] direction the valence electron density displays a turn-over around 7.7 GPa.

d -orbitals, respectively. The electrons displaced from the s , p orbitals may have occupied the $4d_{x^2-y^2}$ and $4d_{z^2}$ orbitals. The assignment is consistent with local T_d point-group symmetry as the d -orbital pair transform as the E representation.

It is prudent to point out that the differences in EDD are typically at the 3%–4% level. This is comparable to the typical uncertainty in determining EDD at high pressures. We argue that the *change* in EDD with pressure can be determined more precisely than the absolute EDD. This is because the experimental conditions at various pressures are almost identical in the pressure range of this study. It is expected that several uncertainties in data corrections (background, polarization, and absorption corrections) will cancel with each other in the subtraction, resulting in much better precision in the EDD differences. This speculation can be quantified. The electron density can be expressed by: $\rho(\vec{r}) = \frac{1}{V} \sum_{\vec{q}} F(\vec{q}) e^{-2\pi i \vec{q} \cdot \vec{r}}$, where $F(\vec{q})$ is the correct structure factor. Systematic errors in structure determination may include multiplicative errors, twinning, overlaps, and background.³⁰ Errors arising from non-linear and non-isomorphisms effects³⁰ are not very significant and not considered here. So, we define an observed structure factor $F'(\vec{q}) = \epsilon(\vec{q})F(\vec{q}) + \delta(\vec{q})$, where $\epsilon(\vec{q})$ and $\delta(\vec{q})$ represent the multiplicative errors and the additive errors, respectively. The additive term from overlaps and background can be ignored, because in our data analysis, we treat each individual reflection separately in peak fitting procedures, with background individually subtracted, and overlapping reflections, if any, omitted. In our high pressure single-crystal experiments, multiplicative errors contain several sources, including diamond diffraction, sample centering, polarization, and absorption corrections. Because of the small pressure range of this study (<12 GPa), the diamond diffraction effects due to internal strains are negligible. Uncertainties arising from centering processes at different pressure points are small because the centering resolution is typically better than 2–3 μm and the sample size ($20 \times 30 \mu\text{m}^2$) is much bigger than the beam size ($5 \times 10 \mu\text{m}^2$ FWHM). Uncertainties in data corrections (polarization and absorption corrections) should remain the same at different pressure points, because the geometrical conditions and the sample configuration remain unchanged in this study (Fig. S1 in the supplementary material²⁴). So, at two different pressure points P_1 and P_2 , the multiplicative term $\epsilon(\vec{q})$ is assumed to be the same. Thus, the difference in experimental electron density between two pressure points can be written as

$$\begin{aligned} \Delta\rho'(\vec{r}) &= \rho'_{P_1}(\vec{r}) - \rho'_{P_2}(\vec{r}) = \frac{1}{V} \sum_{\vec{q}} [F'_{P_1}(\vec{q}) - F'_{P_2}(\vec{q})] e^{-2\pi i \vec{q} \cdot \vec{r}} \\ &\cong \frac{1}{V} \sum_{\vec{q}} \epsilon(\vec{q}) [F_{P_1}(\vec{q}) - F_{P_2}(\vec{q})] e^{-2\pi i \vec{q} \cdot \vec{r}} \\ &= \frac{1}{V} \sum_{\vec{q}} \left\{ \frac{[F'_0(\vec{q}) - F_0(\vec{q})][F_{P_1}(\vec{q}) - F_{P_2}(\vec{q})]}{F_0(\vec{q})} \right. \\ &\quad \left. + [F_{P_1}(\vec{q}) - F_{P_2}(\vec{q})] \right\} e^{-2\pi i \vec{q} \cdot \vec{r}} \\ &= \frac{1}{V} \sum_{\vec{q}} \left\{ \frac{[F'_0(\vec{q}) - F_0(\vec{q})][F_{P_1}(\vec{q}) - F_{P_2}(\vec{q})]}{F_0(\vec{q})} \right\} \\ &\quad \times e^{-2\pi i \vec{q} \cdot \vec{r}} + \Delta\rho(\vec{r}), \end{aligned} \quad (1)$$

where the first and the second terms represent uncertainty and true ΔEDD , respectively. To demonstrate the uncertainty level, we have calculated the term $[F'_0(\vec{q}) - F_0(\vec{q})]/F_0(\vec{q})$ for the experimental structure factor at 0.6 GPa, a pressure close to ambient condition, and compared it to the theoretical structure factor $F_0(\vec{q})$.²⁰ We find that the standard error introduced is 1.7%, with detail numbers listed in Table S3 in the supplementary material.²⁴

The pressure-induced changes in electron density are also displayed in the deformations from spherical atomic electron densities. We have calculated the electron densities, $\Delta\rho = \rho_{obs} - \rho_{cal}$, where ρ_{obs} is the observed electron density and ρ_{cal} is spherical electron density calculated from structure parameters and atomic scattering factors of free atoms.²⁹ The pressure-induced changes in EDD are found to be reproducible in two independent measurements (Fig. S2 in the supplementary material²⁴). At the initial pressure of 1.4 GPa, the 3D $\Delta\rho$ map shows a large ($\sim 10 \text{ e}/\text{\AA}^3$) electron accumulation between two Ge atoms along the [111] displaying a genuine sp^3 hybrid orbitals. This bonding pattern is still clearly visible up to 7.7 GPa. In contrast, above 7.7 GPa, the electron density around Ge nuclei is modified dramatically. The sp^3 bonding along [111] direction is gradually suppressed as the pressure increases, and electrons accumulate along the [100] direction with significant non-spherical charge distortion ($\sim 5 \text{ e}/\text{\AA}^3$) around the Ge nuclei with $d_{x^2-y^2}$ and d_{z^2} characters (Figs. S2(c)–S2(f) in the supplementary material²⁴).

The observed reduction in sp^3 bonding and emergence of d -like orbitals should have a signature in valence band spectrum in XES. For this purpose, we conducted resonant XES (RXES) experiments near the Ge $K\beta_2$ (transition from $4p$ states to $1s$ core state at 11 100.8 eV) at 2.9, 7.7, 10.2, 10.9, 11.6, 12.7, and 13.9 GPa at the HPCAT 16-ID-D (Fig. S3 in the supplementary material²⁴). A standard Mao-Bell piston-cylinder DAC with enlarged side openings and 300 μm flat culet diamonds was used in the experiments. The Ge sample was loaded into a 100 μm diameter hole drilled in a Be gasket. Neon was loaded as a pressure transmitting medium. The incident x-ray energy calibration was monitored *via* x-ray absorption through a Ge foil. The signal from the sample was diffracted by a spherically bent single crystal Si (555) analyzer and collected by an Amptek detector in a Rowland circle geometry.³¹ The combined energy resolution of our RXES experiments is about 1 eV.³² In the RXES measurements, emission spectra were measured at incident energies in 1.5 eV steps from 11 098.0 eV to 11 112.0 eV tuned across the Ge K -edge (11 103 eV). In RXES, the core-hole lifetime broadening can be partly reduced by detuning of the incident photon energy with respect to the resonance energy. Since the lifetime broadening of the final state is considerably smaller than that of the core excited state, the resonant method has a remarkable sharpening effect^{33,34} and significantly enhances footprints of the electronic excitations. The widths of the XES band increase significantly with pressure up to 7.7 GPa and then decrease abruptly or increase slow down until 10 GPa, close to the α - β transition (Fig. 3(a)). For example, the pressure dependence of the RXES spectra with incident energy of 11 112 eV is plotted in Fig. 3(b), and the FWHM (ΔE) values of the valence-band

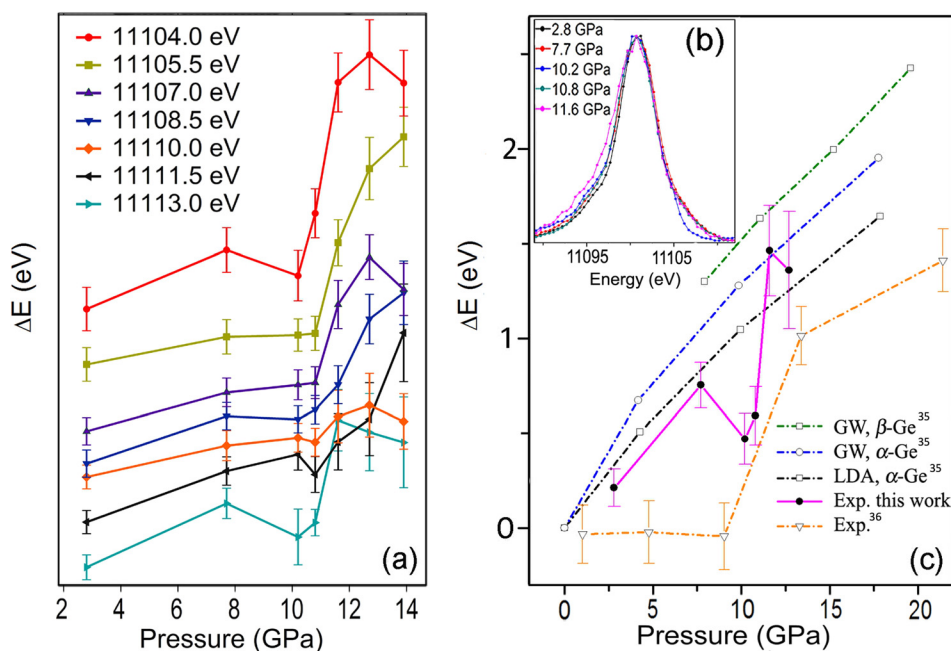


FIG. 3. (a) Changes in the linewidth of the valence band in α -Ge under pressure with various excitation energies. (b) The XES data of α -Ge $K\beta_2$ at high pressures measured with an incident energy of 11113.0 eV. (c) The full width at half maximum of the XES data as a function of pressure, representing the width of valence band (ΔE in eV), which are compared to those of theoretical calculations and the experimental results from the previous studies.^{35,36} Due to the sharpening effect of the resonance XES, we are able to detect the changes in ΔE in α -Ge as a function of pressure.

emission in Fig. 3(c). The measured bandwidths are in good agreement with the LDA calculations but smaller than the GW results.³⁵ From 2.8 GPa to 7.7 GPa, the emission linewidth increased by 0.5 eV. A noticeable drop of 0.3 eV was observed above 7.7 GPa before the phase transition. Between 10 and 11 GPa, the linewidths increase again from 5 eV to 6.5 eV, coinciding with the α - β transition (Fig. 3(b)). According to band structure calculations, the bottom of the valence band at 10 eV below the Fermi level has strong $4s$ contribution, and the highest energy band centered around 2.5 eV from the Fermi level is composed of primarily $4p$ states.^{36,37} The broadening of the valence band width at low pressures can be understood from the expected increase of the dominant p -state band width due to compression. We believe that the sudden reduction in the emission band width above 7.7 GPa with the appearance of d -orbitals in the EDD (Fig. 2) is not a coincidence. It is not unreasonable to postulate that the mixing of d -state at the top of the valence band reduces the intensity of the $4p \rightarrow 1s$ dipole transitions at the higher energy edge of the XES spectra. This corresponds exactly to what we observed in the emission experiment.

The experimental results show clearly that there are pressure induced changes in the electron topology and electronic structure within the stability field of α -Ge below the α - β transition pressure at 11 GPa. It is generally accepted that the metallic character of the β -Ge is related to increased coordination and the strong participation of d -orbitals in the bands.^{7,9} Our view is that, at high pressure, the sp^3 Ge-Ge bonds could be weakened and led to local positional disorder at the Ge symmetry sites. At the same time, this weakening process could promote the hybridization with the $d_{x^2-y^2}$ and d_{z^2} orbitals. This effect is reflected in larger and isotropic displacement parameters (Table S1 in the supplementary material²⁴). A similar effect has been observed and characterized by MEM close to the isostructural transition of $\text{Ba}_8\text{Si}_{46}$ clathrate.³⁸ The observed pressure induced changes in electronic structure may indicate that there is a pre-transition process in Ge. If this is indeed the case, the weakening of the

covalent bonds preceding a structural phase transition could be a general feature in group IV elements (Si, Ge, α -Sn), III-V compounds, and II-VI compounds. This also helps to explain the unexpected discrepancy between theoretically calculated and experimental linewidths in XES, because if the Ge atoms are locally disordered, the assumption of fixed positions in the calculations is no longer valid and will not yield the correct result. Another viewpoint is to explain this phenomenon as the creation of new bonding interactions between second nearest neighbors of the β -Ge at the cost of weakened sp^3 directional bonds with four nearest neighbors.³⁹ The s , p valence electrons initially participated in the localized “chemical bonds” will transfer to spatially extended $4d$ orbitals and eventually responsible for the metallic character of the β -Ge. Above 7.7 GPa, participation of the degenerated $4d_{x^2-y^2}$ and $4d_{z^2}$ orbitals in the valence band increases progressively with increasing pressure. It is not clear how the involvement of the d -orbitals, when at a certain critical level, may trigger the shear distortion of the structure, causing the α - β transition. However, it is likely that, at the α - β transition, the $4d_{x^2-y^2}$ and $4d_{z^2}$ orbitals split into two energy levels, with the former hybridized with the $4s$ and $4p$ orbitals forming the covalent bonds on the ab plane, and the $4d_{z^2}$ orbital dominating the metallic bonding along the c axis.⁹

In summary, we have experimentally determined the EDD of α -Ge at high pressures using single crystal diffraction technique. MEM analysis shows that the sp^3 covalent bonding increases with increasing pressure up to 7.7 GPa, above which an increased participation of d electrons in the valence band occurs. This is supported by the results of XES measurements. The direct observations of the pressure-induced gradual changes in electronic structure suggest that the electronic changes happen at pressures far below the α - β transition pressure, providing a pre-transition process that may be common in other covalent-metallic phase transitions.

Thanks are due to Hui Li for the discussion and data analysis assistance, to Daijo Ikuta, Changyong Park, Yuming

Xiao, and Paul Chow for assistance in experiments. R.L. thanks the China Scholarship Council (CSC) for financial support. G.S. acknowledges the support of DOE Grant Nos. DE-FG02-99ER45775 and DE-NA0001974. The sample and DAC were provided by the 4W2 beamline of BSRF, which was supported by Chinese Academy of Sciences (Grant Nos. KJCX2-SWN20 and KJCX2-SW-N03). This work was performed at HPCAT that is supported by DOE-NNSA under Award No. DE-NA0001974 and DOE-BES under Award No. DE-FG02-99ER45775, with partial instrumentation funding by NSF. We thank S. Tkachev for the help in using the gas-loading system, which is supported by GSECARS and COMPRES. APS is a user facility operated for the DOE Office of Science by ANL under Contract No. DE-AC02-06CH11357.

- ¹J. C. Jamieson, *Science* **139**, 762 (1963).
- ²J. R. Chelikowsky, *Phys. Rev. B* **35**, 1174 (1987).
- ³A. Mujica, *Rev. Mod. Phys.* **75**, 863 (2003).
- ⁴T. Soma, *J. Phys. C: Solid State Phys.* **11**, 2681 (1978).
- ⁵A. Morita and T. Soma, *Solid State Commun.* **11**, 927 (1972).
- ⁶J. Phillips, *Phys. Rev. Lett.* **27**, 1197 (1971).
- ⁷J. Tse and E. Boldyreva, in *Modern Charge-Density Analysis*, edited by C. Gatti and P. Macchi (Springer, The Netherlands, 2012), pp. 573–623.
- ⁸M. T. Yin and M. L. Cohen, *Phys. Rev. Lett.* **50**, 2006 (1983).
- ⁹R. Biswas and M. Kertesz, *Phys. Rev. B* **29**, 1791 (1984).
- ¹⁰A. Mujica, S. Radescu, and R. J. Needs, *J. Phys.: Condens. Matter* **13**, 35 (2001).
- ¹¹M. Durandurdu and D. Drabold, *Phys. Rev. B* **66**, 041201 (2002).
- ¹²C. Menoni, J. Hu, and I. Spain, *Phys. Rev. B* **34**, 362 (1986).
- ¹³N. Bouarissa, A. Tanto, H. Aourag, and T. Bent-Meziane, *Comput. Mater. Sci.* **3**, 430 (1995).
- ¹⁴S. Massidda and A. Baldereschi, *Solid State Commun.* **56**, 431 (1985).
- ¹⁵D. Keating, A. Nunes, B. Batterman, and J. Hastings, *Phys. Rev. B* **4**, 2472 (1971).
- ¹⁶J. B. Roberto, B. W. Batterman, and D. T. Keating, *Phys. Rev. B* **9**, 2590 (1974).
- ¹⁷D. Yoder-Short, R. Colella, and B. Weinstein, *Phys. Rev. Lett.* **49**, 1438 (1982).
- ¹⁸G. Shen, D. Ikuta, S. Sinogeikin, Q. Li, Y. Zhang, and C. Chen, *Phys. Rev. Lett.* **109**, 205503 (2012).
- ¹⁹S. Israel, K. S. Syed Ali, R. A. J. R. Sheeba, and R. Saravanan, *J. Phys. Chem. Solids* **70**, 1185 (2009).
- ²⁰Z. Lu, A. Zunger, and M. Deutsch, *Phys. Rev. B* **47**, 9385 (1993).
- ²¹K. Nakahigashi, K. Higashimine, H. Ishibashi, and S. Minamigawa, *J. Phys. Chem. Solids* **54**, 1543 (1993).
- ²²R. Saravanan, K. S. Syed Ali, and S. Israel, *Pramana* **70**, 679 (2008).
- ²³H. K. Mao, J. Xu, and P. M. Bell, *J. Geophys. Res.: Solid Earth* **91**, 4673 (1986).
- ²⁴See supplementary material at <http://dx.doi.org/10.1063/1.4929368> for experimental configuration, the difference EDD maps, resonant x-ray emission spectra, refinement parameters, and comparison between Fc and Fo.
- ²⁵P. Dera, K. Zhuravlev, V. Prakapenka, M. L. Rivers, G. J. Finkelstein, O. Grubor-Urošević, O. Tschauer, S. M. Clark, and R. T. Downs, *High Pressure Res.* **33**, 466 (2013).
- ²⁶G. Sheldrick, *Acta Crystallogr., Sect. A: Found. Crystallogr.* **64**, 112 (2008).
- ²⁷M. Sakata and M. Sato, *Acta Crystallogr., Sect. A: Found. Crystallogr.* **46**, 263 (1990).
- ²⁸F. Izumi and R. A. Dilanian, *Recent Research Developments in Physics* (Transworld Research Network, Trivandrum, 2002), Vol. 3, pp. 699–726.
- ²⁹K. Momma and F. Izumi, *J. Appl. Crystallogr.* **44**, 1272 (2011).
- ³⁰D. Borek, W. Minor, and Z. Otwinowski, *Acta Crystallogr., Sect. D: Biol. Crystallogr.* **59**, 2031 (2003).
- ³¹H. H. Johann, *Z. Phys.* **69**, 185 (1931).
- ³²Y. M. Xiao, P. Chow, G. Boman, L. G. Bai, E. Rod, A. Bommannavar, C. Kenney-Benson, S. Sinogeikin, and G. Y. Shen, *Rev. Sci. Instrum.* **86**, 072206 (2015).
- ³³A. Kotani and S. Shin, *Rev. Mod. Phys.* **73**, 203 (2001).
- ³⁴J. P. Rueff and A. Shukla, *Rev. Mod. Phys.* **82**, 847 (2010).
- ³⁵P. Modak, A. Svane, N. Christensen, T. Kotani, and M. van Schilfhaar, *Phys. Rev. B* **79**, 153203 (2009).
- ³⁶V. Struzhkin, H. K. Mao, J. F. Lin, R. Hemley, J. Tse, Y. Ma, M. Hu, P. Chow, and C. C. Kao, *Phys. Rev. Lett.* **96**, 137402 (2006).
- ³⁷W. Jank and J. Hafner, *Phys. Rev. B* **41**, 1497 (1990).
- ³⁸J. S. Tse, R. Flacau, S. Desgreniers, T. Iitaka, and J. Z. Jiang, *Phys. Rev. B* **76**, 174109 (2007).
- ³⁹J. Ihm and M. Cohen, *Phys. Rev. B* **23**, 1576 (1981).
- ⁴⁰M. Durandurdu, *Phys. Rev. B* **71**, 054112 (2005).